Supporting Information for

Mapping Orientational Order of Charge-probed Domains in a Semiconducting Polymer

Nicola Martino[1,2], Daniele Fazzi[1,3], Calogero Sciascia[1], Alessandro Luzio[1], Maria Rosa Antognazza[1], Mario Caironi[1,*]

1. Center for Nano Science and Technology @PoliMi, Istituto Italiano di Tecnologia, Via G. Pascoli 70/3, 20133 Milano, Italy

2. Dipartimento di Fisica, Politecnico di Milano, Piazza L. da Vinci, 32, 20133 Milano, Italy

3. Max-Planck-Institut für Kohlenforschung (MPI-KOFO), Kaiser-Wilhelm-Platz 1, D-45470, Mülheim an der Ruhr, Germany.

Supplementary Discussions

Charge density estimation. The number of monomers in the accumulation layer has been estimated considering the molecular weight of a single monomer (986 g/mol) and the density of the polymer (ρ = 1.1 g/cm^3). If the thickness of the channel is d = 2 nm, the number of monomers per unit area of the accumulation layer is N_m = 1.3 x 10^{14} cm^{-2}. The charge superficial density has been calculated from the specific capacitance of the dielectric layer (C = 3.4 nF/cm^2) and the applied gate voltage ($V_g - V_t$ = 25 V) to be N_c = 5.21 x 10^{11} cm^{-2}. From these values, it follows that in the accumulation layer there is, as a first approximation, one charge every 244 monomers of the polymer.

Signals measured by p-CMM. What it's actually collected during the scans in a p-CMM experiment, with the photodiode, is the power of the probe light that, in each pixel of the map, is transmitted through the sample (see Supplementary Figure S2). This signal has two components: a DC component, that is the "usual" transmitted light intensity (T) through the sample and would be the only signal present if there was no modulation applied to the gate of the transistor; from this signal the OD value is calculated as described in the next section. However, since a modulation is applied to the gate electrode, charges are periodically injected in the device and accumulated within the channel. These charges modify the transmission of the semiconducting film as the charged molecules have different optical transitions with respect to the neutral ones. The effect of this modulation on the transmitted light is very small (the modulation is about 10^{-4} with respect to the baseline DC signal), therefore in practice it does not modify the transmission (T) signal. However, it is possible to extract this small AC component, which has the same

frequency of the gate modulation, by means of a lock-in amplifier. The amplitude of this AC component is what is usually referred to as differential transmission (ΔT) in CMS experiments. The final CMS signal is then given by the ratio $\Delta T/T$. After a p-CMM measurement we thus end up with two images: the map of the OD signal and the map of the CMS signal. As explained in the main text, while collected simultaneously, the two maps give fundamentally different information. The OD map is related to the absorption of all the bulk of the material, and thus it conveys information on the mean morphology of the semiconducting layer. The CMS signal, however, arises only from the charged molecules, which are all located at the dielectric interface. So, the information (i.e. the orientation of the polymeric chains) obtained by analyzing the dependence of the CMS signal on laser polarization, are not relative to the entire semiconducting film, but reflect the morphology of only the charged molecules, which are a subset of all the molecules present in the accumulation region

The p-CMM setup is also able to collect local spectra of the CMS signal. In this case, the sample is kept fixed in a position and what is scanned is the wavelength of the probe light (the white-light supercontinuum laser is filtered with an acousto-optic based monochromator). Again, both the T and ΔT at the different wavelengths are collected simultaneously and the CMS spectra is reconstructed as $\Delta T/T$. Local CMS spectra can thus be collected in different point of the sample or in the same point with different probe polarisation states.

Optical density maps. Extracting the value of the semiconducting film optical density (OD) from the intensity of the light transmitted through the device is not straightforward, since one has to take into account different factors than can attenuate the incident light beam, other than the

polymer absorption (e.g. optical losses in the experimental setup, reflections at the different interfaces of the device, scattering losses…). To decouple these effects, we measured the optical density of a thin film of P(NDI2OD-T2) on a glass substrate deposited with the same process as the one used for the active layer in the real transistor used in this study.

The actual macroscopic optical density of the film was obtained by measuring the reflection and transmission spectra of the sample (R_s, T_s) and the glass substrate (R_g, T_g) in a spectrophotometer with an integrating sphere (Perkin Elmer Lambda 1050). The OD spectrum, reported in Supplementary Fig. S3, was calculated as:

$$OD = -log_{10}\left(\frac{T_s(1-R_g)}{(1-R_s)T_g}\right)$$

and an optical density of $OD_M = 0.103$ was extracted at $\lambda = 690$ nm. To obtain the OD maps shown in Figure 2 of the main text and in Supplementary Fig. S6, we hypothesized that in the probed 10x10 μm^2 region of the device domains with all possible orientations are present1; from this it follows that the mean optical density of the semiconducting layer in the probed region should be equal to the one measured macroscopically with the spectrophotometer. To convert from the data of transmitted light intensity $I_{(x,y)}$ in each pixel to the OD maps we then used the following formula:

$$OD_{(x,y)} = OD_M + \langle \log_{10} I_{(x,y)} \rangle - \log_{10} I_{(x,y)}$$

where the brackets stand for the mean value of all the pixels of the map.

The hypothesis of having all the possible orientation in the recorded maps is reasonable for the case of the device casted from dichlorobenzene, since the domains have a limited extension

(from hundreds of nm to few μm). In this case we have many domains with different orientations in a single map (10x10 μm^2, as it can be clearly seen in the maps of Figure 5 of the main text) and the mean absorption of the probed area can thus be effectively considered isotropic and equal to the macroscopic one. However, this assumption cannot be considered valid in the case of the device casted from toluene: even though in this case the maps cover a bigger area (35x35 μm^2), we have only two very big domains. Since in this case we do not have any reliable way to extract the optical density from transmission data, we do not report the OD maps in Figure 6.

CMS of P(NDI2OD-T2). In a CMS experiment, charges injected in a FET accumulation layer induce variations (ΔT) in the optical transmission (T) of the device which are recorded as specific spectral fingerprints of mainly two types: *bleaching features* ($\Delta T/T > 0$), in the regions of the ground state transitions, related to the decreased number of neutral species, and *absorption bands* ($\Delta T/T < 0$) of the charged (polaronic) species. Since the CMS signal arises only from excited-state species, it has an intrinsic sensitivity to probe the optoelectronic properties of the semiconductor regions where the charge transport actually occurs, which in the case of an OFET is a few-nm layer buried at the dielectric interface.

In the case of P(NDI2OD-T2), the CMS spectrum (grey line in Figure 3a of the main text) in the visible/near-infrared region shows two bleaching peaks: the main one, centred at λ = 700 nm, is related to the lower energy electronic transition of the neutral polymer chain (it is the one probed in the text at 690 nm); the secondary bleaching peak at λ = 775 nm is not a vibronic replica, but is instead associated to a different electronic transition, due to the presence of molecular aggregates in the film[2]. The third feature present in the spectrum is a negative band, centred at λ

= 850 nm, attributed to an induced absorption related, as also revealed by quantum-chemical calculations, to one of the electronic transitions of the negatively charged species[3].

Quantum chemical calculations. The oligomer length considered for describing the electronic structure (both neutral and charged species) of P(NDI2OD-T2) consists in four repeat units (n = 4). This length has been previously demonstrated to well reproduce the electronic properties of P(NDI2OD-T2)2,4 and, overall, is sufficiently large for describing the polaronic effects. In fact, the typical polaron relaxation length for P(NDI2OD-T2) is around three repeat4.

A full ground state geometry optimization (without constrains) has been carried out at the restricted CAM-B3LYP/6-31G** level of theory for describing neutral species. The charged state (extra electron) has been described as the anion species (-1 charge) at the UCAM-B3LYP/6-31G** level of theory. Cartesian coordinate, total SCF energy and spin contamination of the two geometries are reported in Supplementary Tables S1 and S2.

Vertical excitations (ground to excited states transitions) have been computed at the TD-CAM-B3LYP/6-31G** level of theory. Although it is well known5 hat CAM-B3LYP overestimates the vertical excitation energies (especially if compared to other DFT functionals as PBE0 or B3LYP), it well describes the charge-transfer (CT) state character thus being necessary for the case of P(NDI2OD-T2). Indeed, as already proofed2,4, the first excited state (i.e. S_1) has a strong component of *intra*-molecular CT character.

However, for a better and complete comparison, in the case of the neutral molecule we report the vertical excitation energies computed with the B3LYP and with the CAM-B3LYP functional

(Supplementary Tables S3 and S4 respectively), while for the charged case only the CAM-B3LYP functional is reported (Supplementary Table S5).

Regarding the neutral species, the main character of $S_0 \rightarrow S_1$ transition (that is the bleaching peak probed at $\lambda = 690$ nm in the main text) is, for both DFT functionals, the HOMO → LUMO single-particle excitation, being the HOMO mainly localized on the T2 moiety and the LUMO on the NDI2OD (i.e. intra-molecular CT excitation). Despite CAM-B3LYP overestimate the $S_0 \rightarrow S_1$ excitation energy with respect to B3LYP (more close to the experimental data), the assignment of the excitation is correct. On the other side, CAM-B3LYP properly describes the excited state transition of the charged species while B3LYP underestimate the energies due to the lack in the long-range energy screening6.

For the charged species, the electronic transition associated to the CMS absorption band (probed at $\lambda = 870$ nm) is the $S^-_0 \rightarrow S^-_6$ one. Even in this case CAM-B3LYP overestimates the vertical energy but it properly describes the character of the excitation. The $S^-_0 \rightarrow S^-_6$ single molecular orbital contributions (SOMO) are reported in Supplementary Table S6, where the 470A is the SOMOα. A full list of the single occupied molecular orbitals involved in the transition is reported in Supplementary Table S7. The main contribution to the excited state wavefunction comes from the 470 → 485 transition, featuring an intra-molecular CT character. 470 orbital is mainly localized on the NDI2OD unit while the 485 is more delocalized on the T2 one. Possible explanations for the overestimation of the computed excited state energy if compared to the experimental value are: 1) the DFT functional (ongoing are further investigations about a full DFT screening for the charged states) and 2) the oligomer length (i.e. the electron delocalization). To give insights about the second point, we report also the excitation energies for the charged species of a five repeat units oligomer (Supplementary Table S8). The active

excitation shifts from 1.83 eV for n = 4 to 1.79 eV for n = 5. Even for the n = 5 oligomer case, the excited state description is the same as for the n = 4 thus strengthening our assignment.

DFT/TDDFT calculation on a molecular dimer. To gain insights in the role played by *inter*-molecular interaction (even if it is out of the scope of the current work) and to discriminate whether the CMS absorption band is mainly due to *intra*- or *inter*-molecular excited states transition in the charged species, a full DFT optimization and TDDFT calculation has been carried out for a molecular dimer (named *AB*) of P(NDI2OD-T2) featuring one repeat unit per monomer.

The following steps have been carried out:

- full DFT geometry optimization of the neutral molecular dimer;
- TD-DFT calculations for the neutral molecular dimer.
- full DFT geometry optimization of the charged (-1) molecular dimer;
- TD-DFT calculations for the charged molecular dimer.

DFT geometry optimization for the neutral/charged molecular dimer have been performed at the M062X / UM062X/6-311G** level of theory, TDDFT calculations for vertical excitations at the CAM-B3LYP / UCAM-B3LYP/6-31G** level of theory. In Supplementary Table S9 are reported the figure of the optimized charged molecular dimer (*AB*). Vertical excitations for the neutral and charged **molecular dimer *AB*** (TD-(U)CAM-B3LYP/6-31G**) can be found in Supplementary Table S10. Vertical excitations for the charged **molecular monomer *A*** (TD-UCAM-B3LYP/6-31G**) as extracted from the *AB* geometry are reported in Supplementary Table S11.

A full detail spectroscopic work and assignment will be reported elsewhere. However, the relevant point emerging from this investigation is that the main excitation has a strong *intra*-molecular character. In fact, the optical allowed transition associated to the CMS band (870 nm) is in the dimer the $S^-_0 \rightarrow S^-_2$ at 1.79 eV and in the monomer the $S^-_0 \rightarrow S^-_2$ at 2.03 eV. A small shift is present due to the intermolecular Van der Waals interaction but the character of the transition is preferentially *intra*-molecular, as clearly shown by the molecular orbitals involved in the transitions (Supplementary Tables S12 and S13). The same picture emerges for the neutral case where the $S_0 \rightarrow S_1$ transition in the dimer and in the monomer are similar.

In this frame, the orientational/directional order information derived from p-CMM maps is independent from the real nature of the polaron, i.e. whether it is delocalised over adjacent polymer chains or if it is localised over one.

Supplementary References

1. Sciascia, C. *et al.* Sub-micrometer charge modulation microscopy of a high mobility polymeric n-channel field-effect transistor. *Adv. Mater.* **23**, 5086–5090 (2011).
2. Steyrleuthner, R. *et al.* Aggregation in a high-mobility n-type low-bandgap copolymer with implications on semicrystalline morphology. *J. Am. Chem. Soc.* **134**, 18303–18317 (2012).
3. Caironi, M. *et al.* Very Low Degree of Energetic Disorder as the Origin of High Mobility in an n-channel Polymer Semiconductor. *Adv. Funct. Mater.* **21**, 3371-3381 (2011).

4. Fazzi, D., Caironi, M. & Castiglioni, C. Quantum-chemical insights into the prediction of charge transport parameters for a naphthalenetetracarboxydiimide-based copolymer with enhanced electron mobility. *J. Am. Chem. Soc.* **133**, 19056–9 (2011).

5. Jacquemin, D., Mennucci, B. & Adamo, C. Excited-state calculations with TD-DFT: from benchmarks to simulations in complex environments. *PCCP* **13**, 16987–98 (2011).

6. Nayyar, I. H. *et al.* Localization of Electronic Excitations in Conjugated Polymers Studied by DFT. *J. Phys. Chem. Lett.* **2**, (2011).

Supplementary Figures

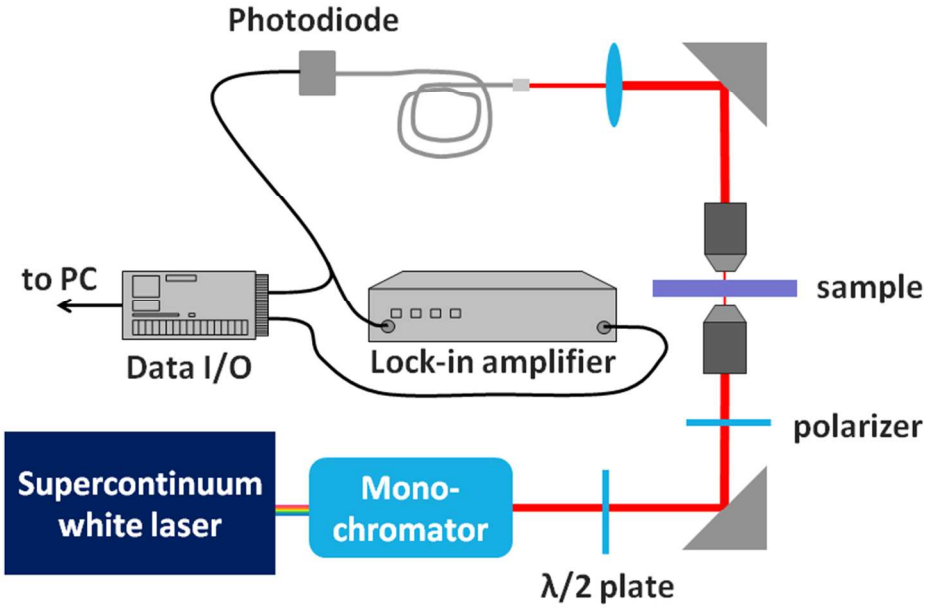

Figure S1. Schematic representation of the experimental setup used for polarised Charge Modulation Microscopy measurements. The addition of the polariser and the $\lambda/2$ plate allows a precise control of the polarisation of the probe light incident on the sample. The source of the probe light is a supercontinuum white-light laser, which has an emission spanning from 475 nm to about 2.5 μm; the probe light is then monochromated by means of an acousto-optic filter. The sample is kept in a custom-made chamber that allow nitrogen flux to avoid degradation of the electrical performance of the transistor.

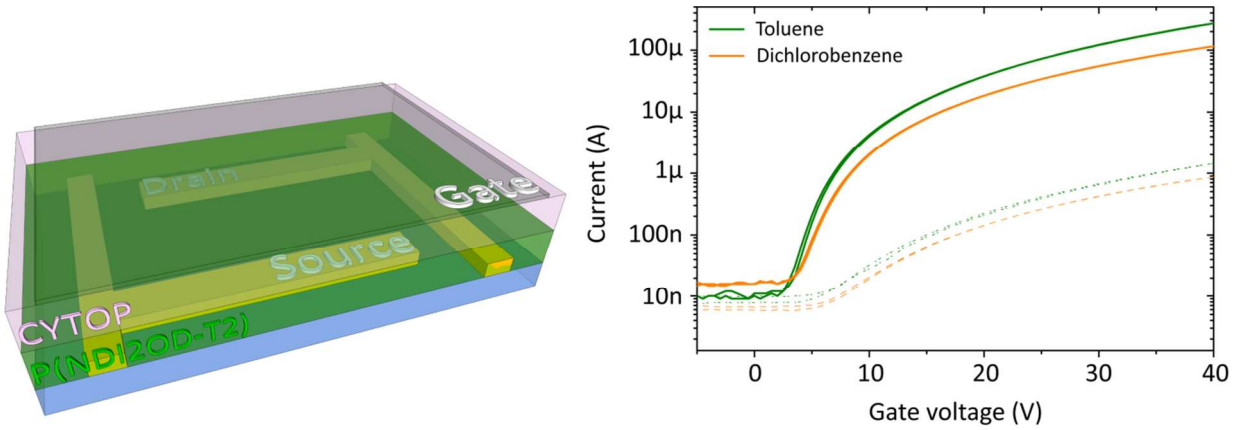

Figure S2. **Device schematization and electrical characterisation.** Left: schematic representation (figure is not drawn to scale) of the top-gate, bottom-contacts FETs realized in this work; channel width W = 20 mm, channel length L = 40 µm, dielectric specific capacitance C_{die} = 4.1 nFcm^{-2}. Right: *n*-channel transfer characteristics in saturation regime (V_d = 40 V) of the organic FETs with P(NDI2OD-T2) films as the active layer deposited by toluene (green line) and dichlorobenzene (orange line) (right); in the plot, the correspondent leakage currents (dotted lines) are also reported. Saturation mobility values of ~ 0.8 cm^{2}V^{-1}s^{-1} and ~ 0.1 cm^{2}V^{-1}s^{-1} were extracted from the transfer curves of P(NDI2OD-T2) films from toluene and dichlorobenzene, respectively.

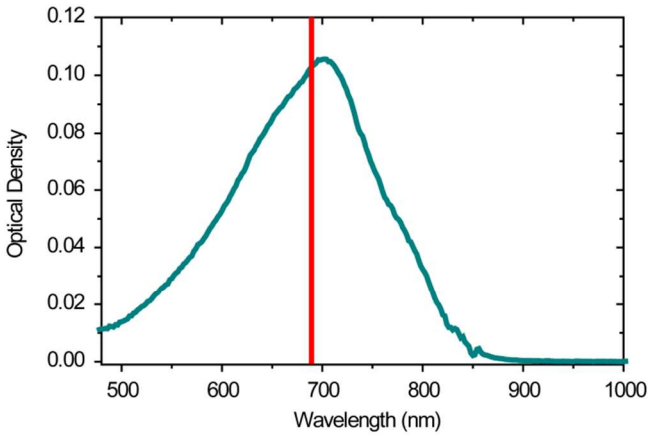

Figure S3. OD spectrum of a thin film of P(NDI2OD-T2) deposited on glass with the same processing parameter used for the fabrication of the real device. From the data we can extract an optical density of 0.103 at λ = 690 nm, where the p-CMM maps presented in the main text have been measured.

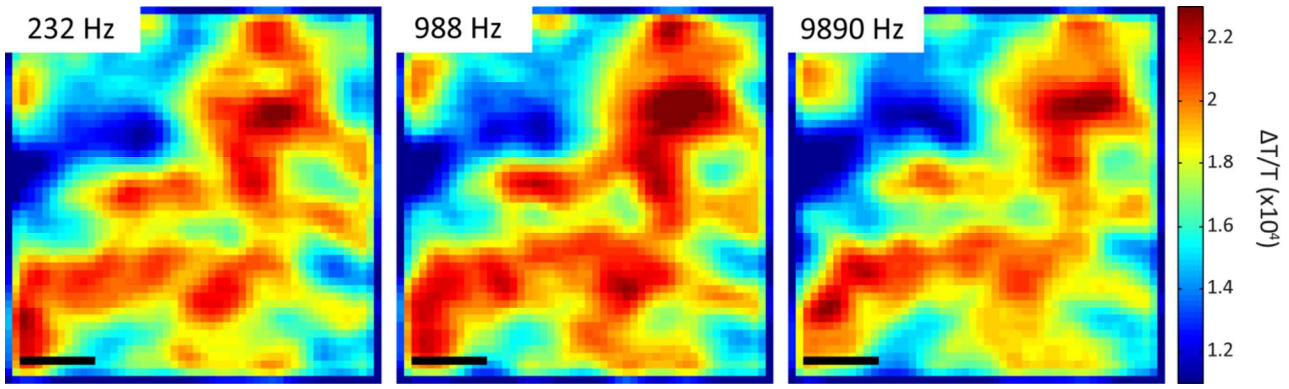

Figure S4. p-CMM signal frequency dependence. 5x5 μm^2 p-CMM maps (probe beam at λ = 690 nm) taken in the same area at different frequencies of the gate voltage modulation between 200 Hz and 10 kHz. Scale bar is 1 μm. The substantial equivalence of p-CMM maps at the different frequencies is a clear evidence that probed carriers are fast enough to respond to variations in the gate voltage and to produce a CMS signal which is synchronous to the modulation frequency in the reported range. Trapped carriers are too slow and cannot contribute to the p-CMM map, even at 232 Hz. These data are consistent with the cut-off frequency of the device which depends on the carriers mobility and channel length, which we have independently estimated to be around 100 kHz.

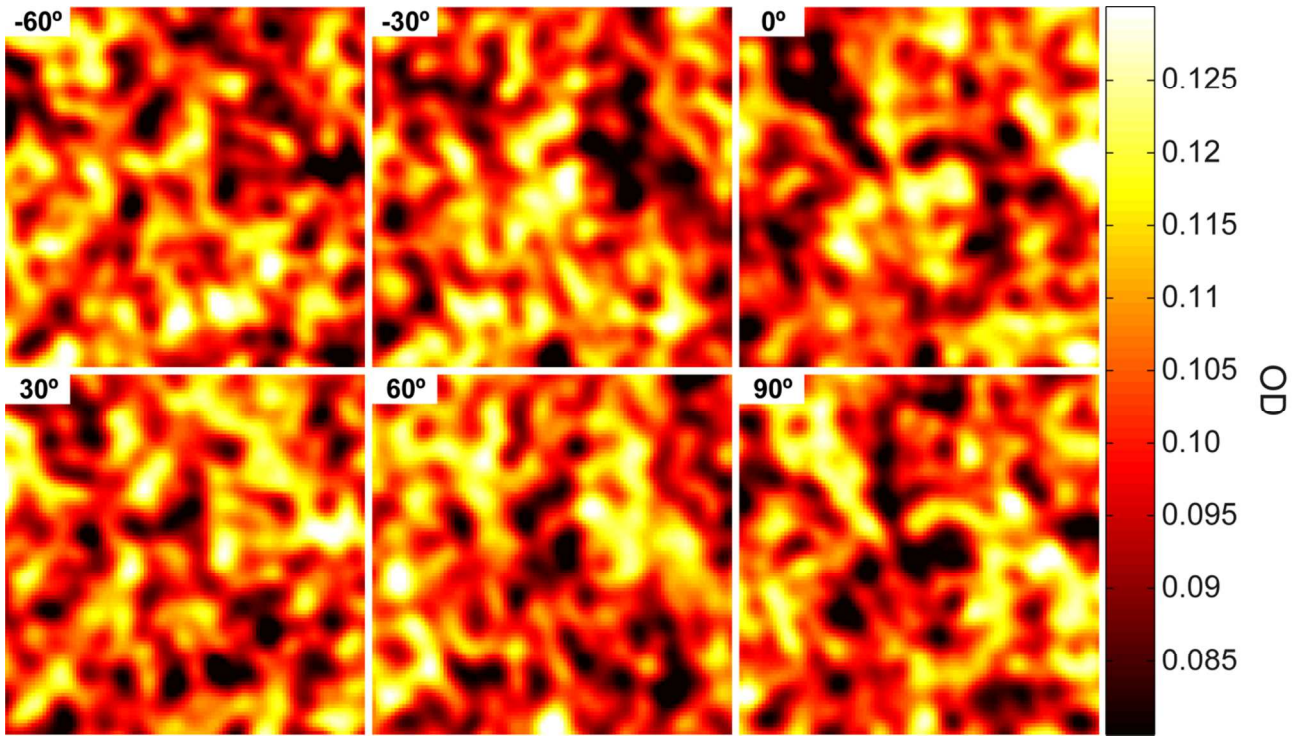

Figure S5. Angular dependence of OD maps. 10x10 μm^2 OD maps taken at 6 different values of the probe light (λ = 690 nm) polarisation (θ) on a device with a P(NDI2OD-T2) semiconductor film deposited from dichlorobenzene. These maps have been calculated from the transmission data with the procedure described in the Supplementary Discussions and then fitted with the quantitative analysis described in the main text to give the results reported in Figure 5 and Supplementary Figure S7 (top panels).

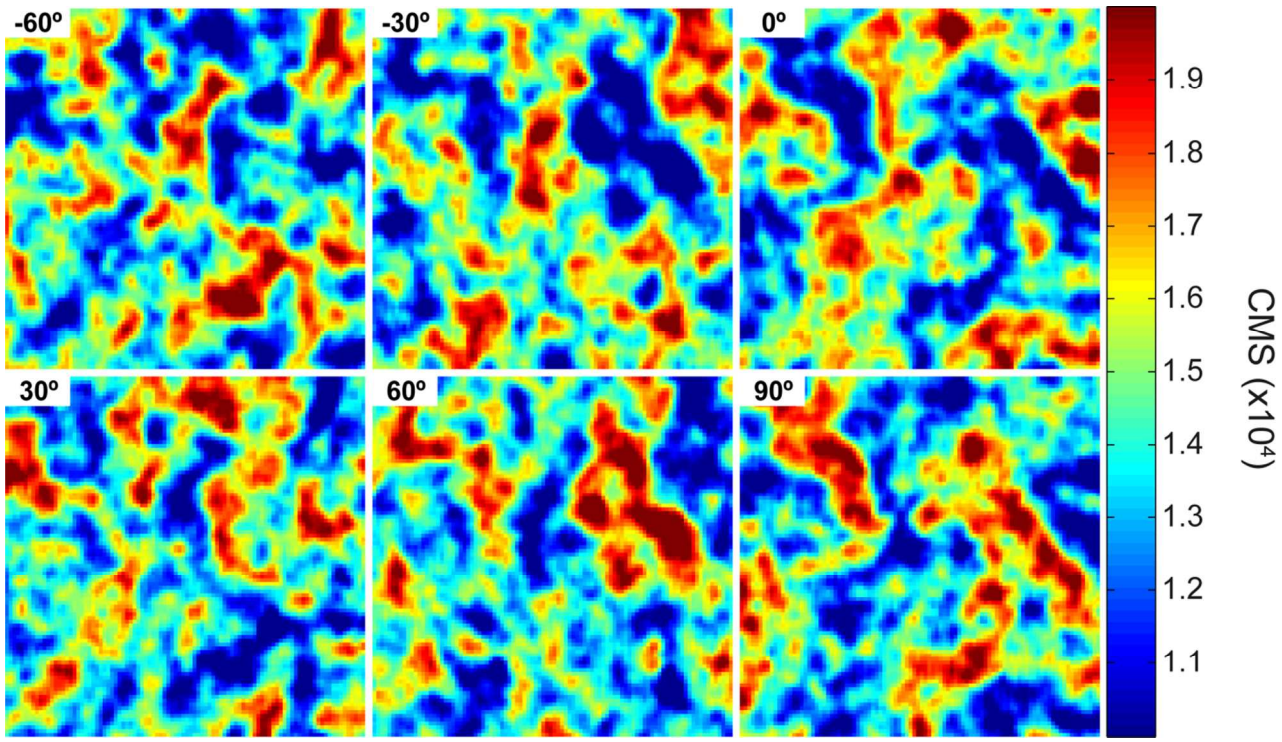

Figure S6. Angular dependence of CMS maps. 10x10 μm^2 CMS (i.e. ΔT/T) maps taken at 6 different values of the probe light (λ = 690 nm) polarisation (θ) on a device with a pristine P(NDI2OD-T2) semiconductor film. These maps have been fitted with the quantitative analysis described in the main text and Supplementary Discussion to give the results reported in Figure 4 and Supplementary Figure S7 (bottom panels).

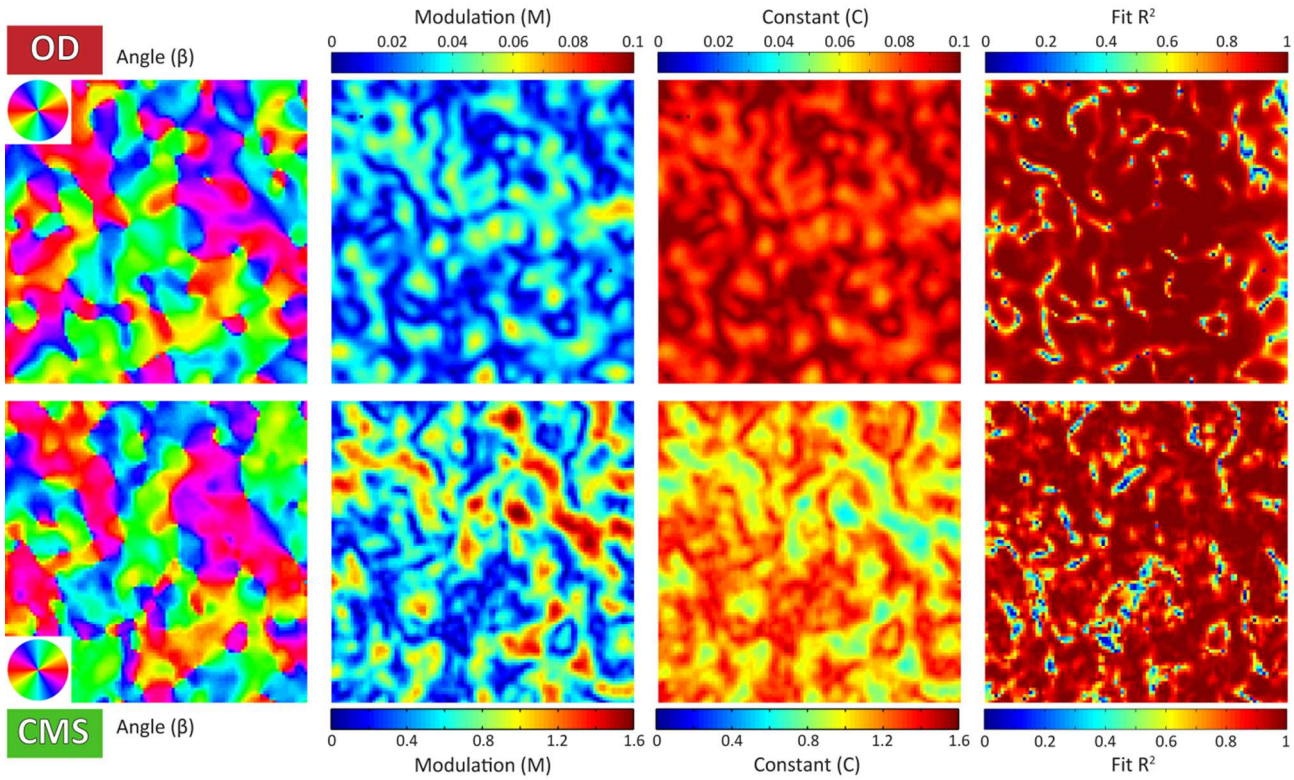

Figure S7. Results of quantitative analysis of p-CMM maps. Results of the quantitative analysis performed on the angular-dependent OD maps (top row) and CMM maps (bottom row) reported in Supplementary Figure S5 and S6 respectively. Angular maps (first column) indicate the preferential orientation of the polymeric backbones in each pixel of the investigated area, while the intensity of the M maps (second column) is related to the number of molecules actually oriented along that direction. The intensity of the C maps (third column) is instead given by the fraction of molecules that produce an isotropic absorption. In the fourth column the value of the R^2 of the fit is reported. It can be seen that the value is almost everywhere close to 1 (indicating a good fitting of the experimental data with the model), except for the boundaries between domains of different alignment; in this case the finite dimension of the probe beam mediates regions with different orientation and the modulation is cancelled out, fading into the experimental error.

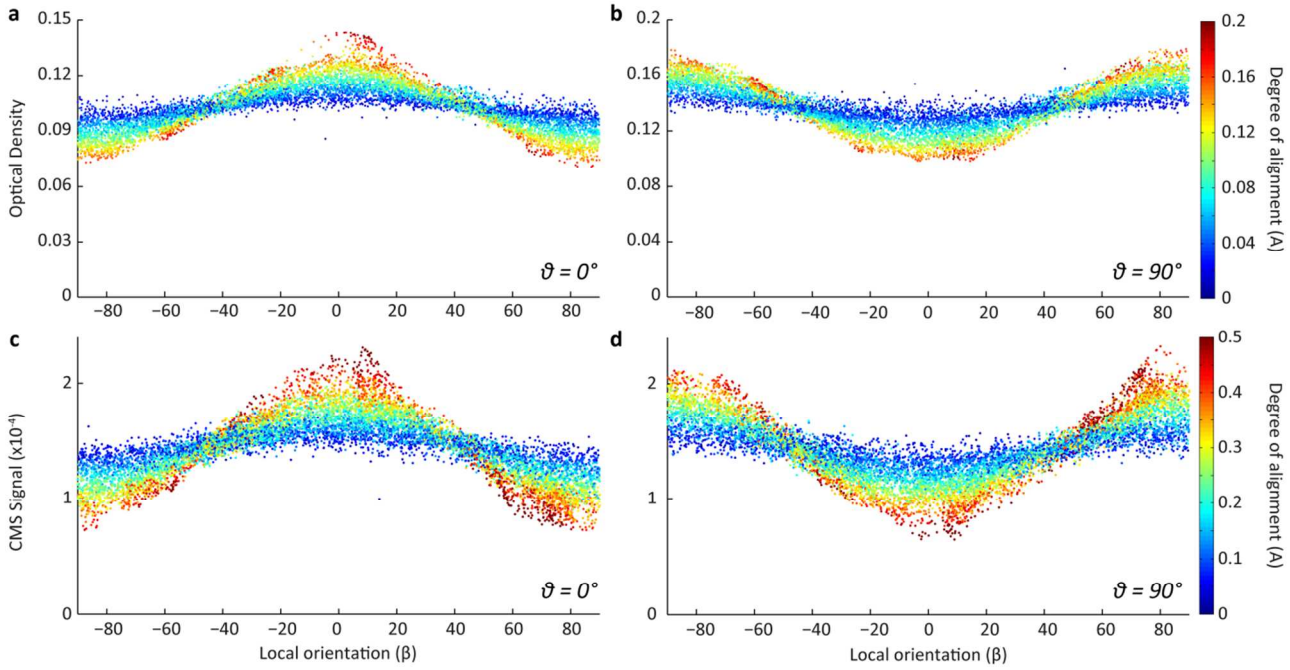

Figure S8. Influence of the degree of alignment on the statistical distribution of p-CMM data. Scatter plots of the OD signal intensity versus the local preferential orientation of the polymeric chains (taken from the β maps), for different laser polarisations: a) $\theta = 0°$, b) $\theta = 90°$; the different points are colour-coded with respect to the local degree of alignment. As expected, points with higher degree of alignment have more pronounced dependence on the orientation angle β. The same analysis has been carried out also for CMS signals (panels c,d); in this case, the angular dependence is decisively more pronounced.

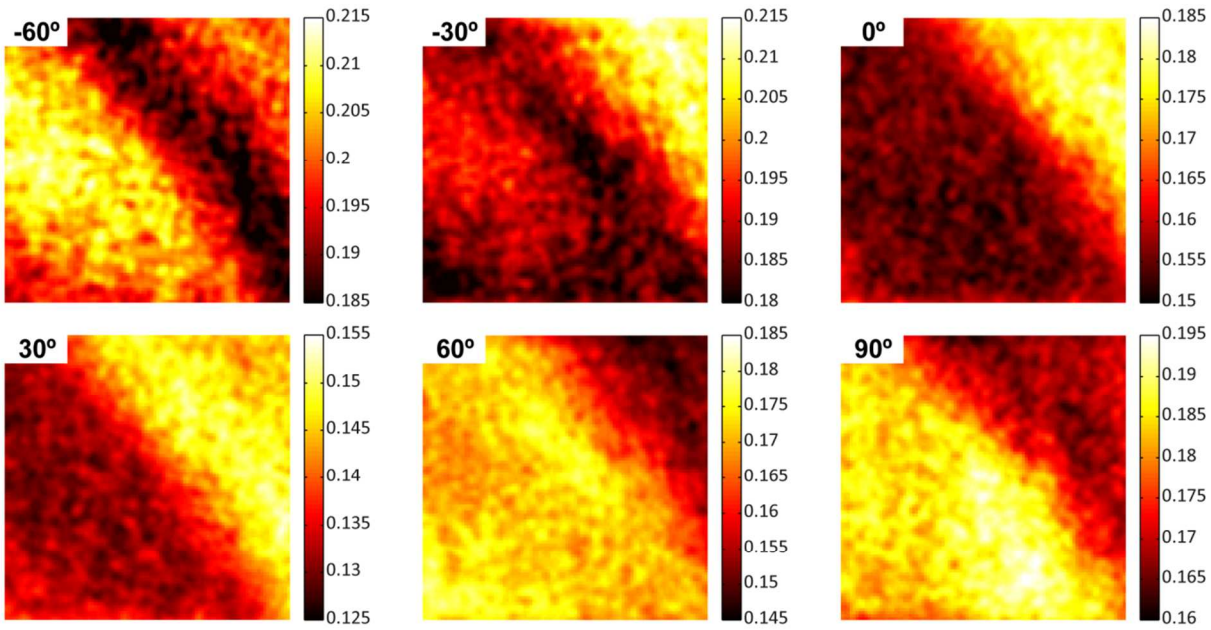

Figure S9. Angular dependence of the transmission data on toluene device. 35x35 μm^2 maps of the raw transmission signal (T) taken at 6 different values of the probe light (λ = 690 nm) polarisation (θ) on a device with a P(NDI2OD-T2) semiconductor film deposited from toluene. As explained in the Supplementary Discussions, unlike the case of the DCB device, the OD data could not be extracted from these maps. Colorscale is in arbitrary units.

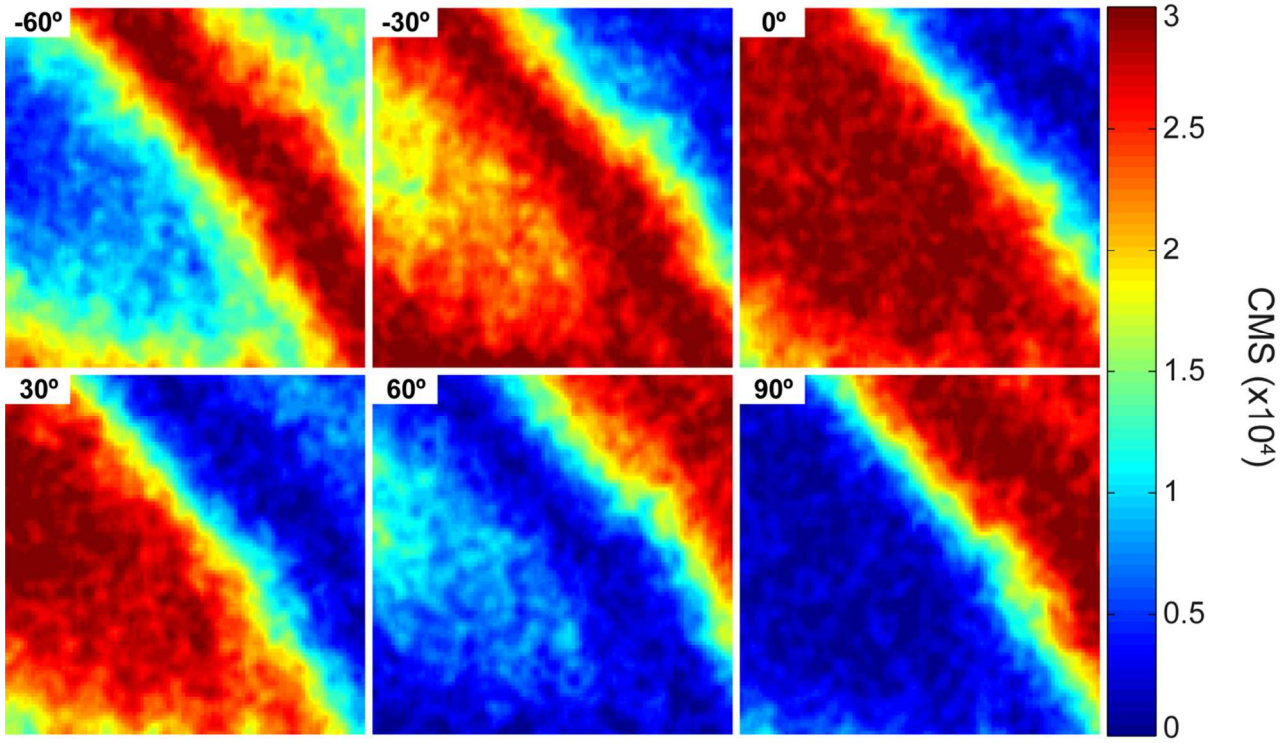

Figure S10. Angular dependence of CMS maps of toluene device. 35x35 μm^2 CMS maps taken at 6 different values of the probe light (λ = 690 nm) polarisation (θ) on a device with a P(NDI2OD-T2) semiconductor film deposited from toluene. These maps have been fitted with the quantitative analysis described in the main text to give the results reported in Figure 6 and Supplementary Figure S11.

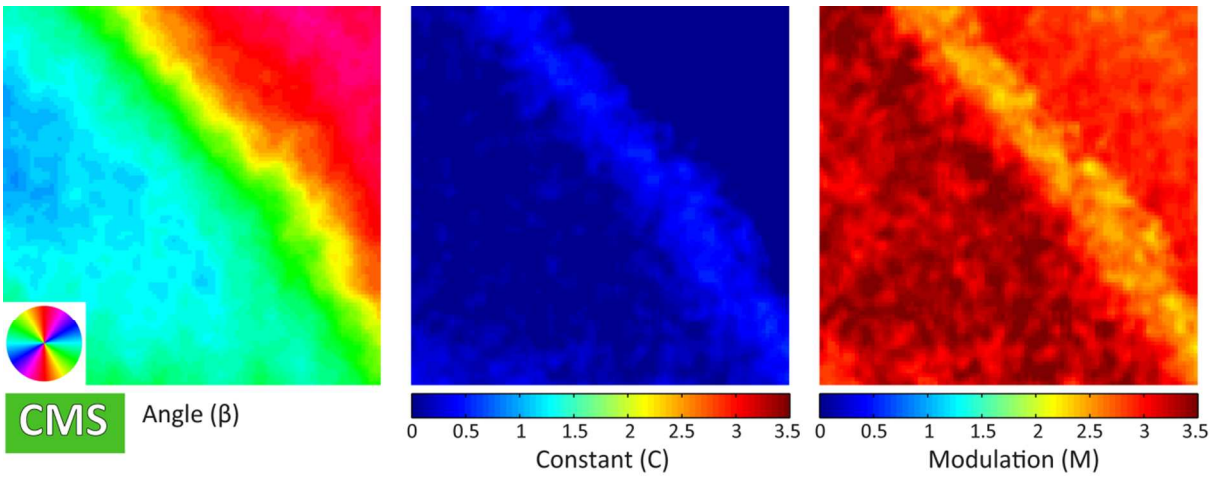

Figure S11. Results of statistical analysis on toluene device. Results of the statistical analysis performed on the angular-dependent 35x35 μm^2 CMS maps reported in Supplementary Figure S10 for a toluene-deposited P(NDI2OD-T2) transistor.

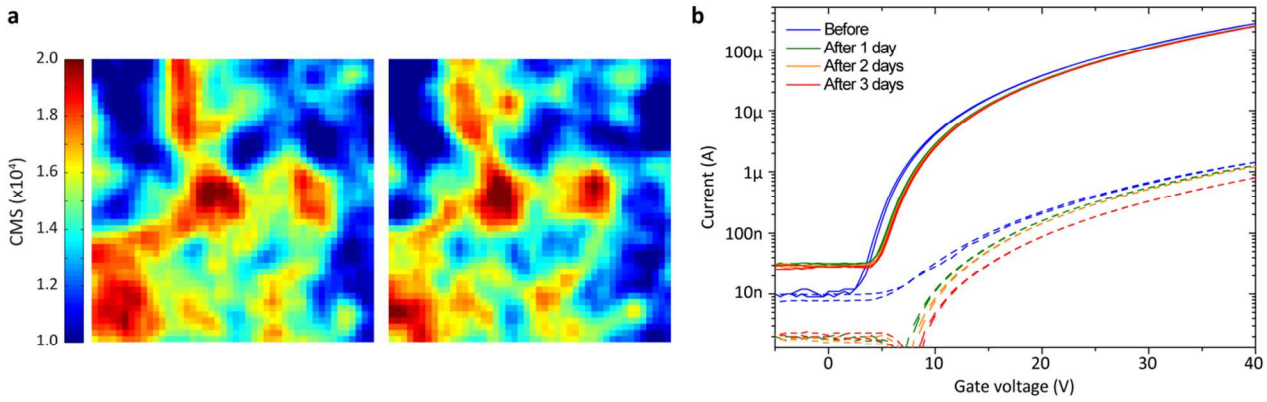

Figure S12. Stability of the device during measurement. p-CMM is a non-invasive and non-destructive technique, both in terms of the optical signal and the electrical stability of the device. a) Two CMS maps of the same 5x5 μm^2 area of the device; the first one is taken just after mounting the sample in the microscope, while the second is taken after the device has been repeatedly measured in that same area for about 8 hours. No significant variations in the intensity of the signal or in the morphological features are visible. b) n-channel transfer characteristics of the transistor as mounted on the microscope (blue line) and after 1, 2 and 3 days of repeated measurements (respectively green, orange and red lines); after an initial slight decrease, the performances of the device remain very stable throughout all the experiment (solid lines are the drain-source currents, dotted lines are the leakage currents).

Supplementary Tables

Table S1. Optimized Cartesian geometry (CAM-B3LYP/6-31G**) for $(NDI2OD\text{-}T2)_4$, neutral species

CAM-B3LYP/6-31G** neutral species			
C	-18.950637	-0.640529	0.214004
C	-18.032248	-1.706346	0.33806
C	-16.707723	-1.458619	0.584719
C	-16.198525	-0.146151	0.739707
C	-17.093773	0.917468	0.670237
C	-18.463758	0.673662	0.389962
C	-19.38233	1.739298	0.266116
C	-20.706876	1.491173	0.019449
C	-21.21645	0.178732	-0.134554
C	-20.320823	-0.884373	-0.065294
C	-16.676088	2.316487	0.975975
N	-17.610041	3.334853	0.766677
C	-18.944257	3.147814	0.423733
C	-20.739059	-2.283892	-0.369153
N	-19.804861	-3.302391	-0.159735
C	-18.470758	-3.115221	0.181864
O	-19.706875	4.083089	0.276958
O	-15.576831	2.60475	1.402793
O	-21.83856	-2.572045	-0.794434
O	-17.707686	-4.050031	0.329548
C	-17.138854	4.695647	1.018485
C	-20.277105	-4.663364	-0.409172
H	-16.029066	-2.301337	0.64296
H	-21.172723	-4.852556	0.183371
H	-20.530905	-4.784221	-1.464011
H	-19.478332	-5.345446	-0.131235
H	-17.939019	5.37745	0.743895
H	-16.882779	4.814174	2.073026
H	-16.24491	4.887742	0.424283
H	-21.385688	2.333731	-0.03914
C	-22.676954	0.079331	-0.327495
C	-23.40657	0.723533	-1.286208
C	-24.807655	0.553721	-1.136861
C	-25.144209	-0.197591	-0.043562
S	-23.720875	-0.732057	0.796316

C	-26.468366	-0.557336	0.437347
C	-26.851786	-0.906435	1.703923
C	-28.242108	-1.189347	1.812088
C	-28.898892	-1.050434	0.628814
S	-27.831664	-0.586953	-0.643352
H	-22.951319	1.300746	-2.082775
H	-25.541971	0.993982	-1.801135
H	-26.162585	-0.940594	2.539885
H	-28.728373	-1.476034	2.736764
H	-29.950693	-1.196616	0.427074
C	-14.738968	-0.046761	0.93565
C	-14.010666	-0.692431	1.895175
C	-12.611359	-0.497791	1.7653
C	-12.275062	0.270949	0.683829
S	-13.694278	0.765436	-0.185684
C	-10.953965	0.672829	0.231521
C	-10.604516	1.769137	-0.509631
C	-9.20777	1.86001	-0.743551
C	-8.500221	0.821795	-0.207188
S	-9.554248	-0.278659	0.621678
C	-7.028333	0.702823	-0.164996
C	-6.276246	-0.359935	-0.655695
C	-4.868613	-0.375787	-0.473845
C	-4.204461	0.690242	0.17222
C	-4.983819	1.778969	0.621307
C	-6.344321	1.773897	0.459679
C	-4.089077	-1.464389	-0.923092
C	-2.728335	-1.458424	-0.763144
C	-2.044385	-0.386629	-0.13973
C	-2.796731	0.674971	0.352981
C	-4.717215	-2.627156	-1.597741
C	-6.896251	-1.455838	-1.456137
N	-6.087639	-2.538147	-1.813426
C	-4.355688	2.941496	1.296435
C	-2.176646	1.770327	1.154158
N	-2.985259	2.852567	1.511846
C	-6.750939	-3.617175	-2.543841
C	-2.321999	3.931193	2.242873
O	-5.000837	3.908241	1.652602
O	-1.017121	1.757363	1.512287
O	-8.05598	-1.443402	-1.813714
O	-4.072161	-3.594131	-1.953405
H	-2.161317	-2.298713	-1.146091

H	-6.911128	2.614722	0.841723
H	-11.322703	2.504937	-0.851667
H	-8.740457	2.667053	-1.295901
H	-14.46747	-1.270925	2.689849
H	-11.880079	-0.89688	2.458306
H	-3.047553	4.72723	2.385705
H	-1.963842	3.564728	3.206733
H	-1.464615	4.286107	1.670156
H	-7.607854	-3.972344	-1.970572
H	-7.109801	-3.251001	-3.507543
H	-6.025171	-4.412965	-2.686943
C	-0.572067	-0.500953	-0.102862
C	0.142821	-1.535035	0.431617
C	1.53831	-1.436978	0.192289
C	1.879182	-0.339506	-0.551091
S	0.472993	0.604223	-0.936736
C	3.195908	0.070323	-1.009115
C	3.522206	0.83506	-2.096453
C	4.91916	1.042569	-2.2307
C	5.6561	0.410784	-1.268426
S	4.621824	-0.404857	-0.139805
H	-0.318083	-2.343929	0.986647
H	2.261753	-2.168617	0.532176
H	2.785437	1.222291	-2.790375
H	5.368583	1.620428	-3.030016
C	7.114406	0.529836	-1.075769
C	8.026496	-0.51887	-0.997023
C	9.391646	-0.252354	-0.716997
C	9.868527	1.06815	-0.552694
C	8.93275	2.116105	-0.704599
C	7.609921	1.847605	-0.942216
C	10.322945	-1.306212	-0.592856
C	11.632723	-1.044668	-0.303591
C	12.133707	0.270899	-0.116466
C	11.236739	1.334029	-0.260232
C	9.346374	3.534747	-0.604301
C	11.667209	2.762665	-0.185566
N	10.69688	3.753297	-0.371532
C	7.627566	-1.924706	-1.296854
C	9.908551	-2.72184	-0.756335
N	8.577924	-2.929432	-1.097419
O	6.529012	-2.229425	-1.714015
O	10.687627	-3.644473	-0.615785

O	8.557035	4.451628	-0.728294
O	12.811391	3.115572	0.01643
C	8.126616	-4.296589	-1.350753
C	11.174616	5.132783	-0.292245
H	6.923897	2.683263	-1.013968
H	12.298792	-1.891611	-0.189444
H	7.859761	-4.413517	-2.402748
H	8.941411	-4.966141	-1.089341
H	7.243329	-4.507124	-0.746873
H	10.321214	5.78548	-0.453543
H	11.617658	5.316122	0.687898
H	11.939337	5.302926	-1.051364
C	13.56374	0.359616	0.226719
C	14.193703	1.034201	1.235583
C	15.57713	0.753909	1.326469
C	16.016791	-0.133163	0.37833
S	14.706463	-0.63531	-0.639048
C	17.363548	-0.627452	0.152726
C	17.754473	-1.800536	-0.434597
C	19.16397	-1.964343	-0.467023
C	19.842365	-0.907365	0.068956
S	18.744437	0.302117	0.649931
H	13.67908	1.714101	1.899638
H	16.227712	1.183574	2.079269
H	17.053413	-2.537056	-0.809524
H	19.66078	-2.833894	-0.881342
C	21.302006	-0.820902	0.287855
C	21.856386	-1.807493	1.142608
C	23.187003	-1.818612	1.469092
C	24.044224	-0.820048	0.964715
C	23.519872	0.162454	0.098395
C	22.144551	0.145907	-0.25291
C	24.396948	1.155497	-0.397341
C	25.726203	1.162543	-0.040057
C	26.24078	0.178394	0.819879
C	25.411055	-0.800305	1.313872
C	25.957693	-1.841904	2.219623
C	23.71071	-2.87666	2.373306
C	23.899836	2.210248	-1.31377
C	21.666495	1.128974	-1.268484
N	25.070115	-2.811371	2.686021
N	22.560459	2.121031	-1.680958
O	20.554294	1.09789	-1.753346

O	24.621341	3.095152	-1.73147
O	22.996137	-3.752819	2.817785
O	27.126275	-1.868574	2.551937
H	21.209411	-2.567605	1.564675
H	27.286383	0.17176	1.105646
H	26.36156	1.944613	-0.439481
C	22.034085	3.094083	-2.637082
C	25.634065	-3.82721	3.572982
H	21.136794	3.559278	-2.227615
H	22.80814	3.836096	-2.812212
H	21.766897	2.594532	-3.570155
H	24.833653	-4.508746	3.847464
H	26.434347	-4.362086	3.059091
H	26.053157	-3.35065	4.460667
SCF Energy = -8513.09913453 Hartree			
Spin Contamination <S2> = 0.0			

Table S2. Optimized Cartesian geometry (UCAM-B3LYP/6-31G**) for $(NDI2OD\text{-}T2)_4$, charged species

UCAM-B3LYP/6-31G** charged (anion) species			
C	-18.893853	-0.9508	0.483448
C	-17.935167	-1.846318	1.0081
C	-16.63378	-1.453394	1.173929
C	-16.187467	-0.148154	0.848139
C	-17.127014	0.767501	0.382064
C	-18.473171	0.363177	0.180553
C	-19.431619	1.258486	-0.342519
C	-20.732445	0.863156	-0.515668
C	-21.17495	-0.442616	-0.196424
C	-20.238438	-1.355379	0.279625
C	-16.787447	2.205115	0.176425
N	-17.756173	3.025079	-0.412002
C	-19.063654	2.65167	-0.695973
C	-20.585547	-2.788889	0.50376
N	-19.616054	-3.609532	1.085717
C	-18.305494	-3.237475	1.366025
O	-19.861308	3.425688	-1.189596
O	-15.72583	2.693094	0.503919
O	-21.657661	-3.269387	0.198079
O	-17.511023	-4.012356	1.861877
C	-17.357023	4.410158	-0.655293
C	-20.018625	-4.99146	1.340351
H	-15.920413	-2.17866	1.547118
H	-20.916918	-5.002306	1.958726
H	-20.24407	-5.494567	0.398214
H	-19.194878	-5.486321	1.847398
H	-18.172455	4.900876	-1.179521
H	-17.155258	4.913692	0.292054
H	-16.445448	4.427055	-1.253486
H	-21.444006	1.587164	-0.894648
C	-22.618904	-0.69377	-0.383793
C	-23.322053	-0.527008	-1.542409
C	-24.721213	-0.707777	-1.382807
C	-25.083668	-0.984815	-0.092858
S	-23.685674	-1.05483	0.936143
C	-26.415371	-1.205274	0.447931
C	-26.853239	-1.044955	1.734585
C	-28.233663	-1.348537	1.900475
C	-28.829128	-1.733632	0.739596

S	-27.71375	-1.74888	-0.575217
H	-22.849217	-0.28616	-2.487509
H	-25.436906	-0.610915	-2.190805
H	-26.210663	-0.700073	2.536524
H	-28.75739	-1.273428	2.845911
H	-29.860608	-2.013609	0.578334
C	-14.741726	0.091298	1.009849
C	-14.007019	-0.144319	2.138368
C	-12.616571	0.07201	1.960561
C	-12.288666	0.438728	0.682596
S	-13.707937	0.525295	-0.31466
C	-10.97797	0.727608	0.127518
C	-10.66846	1.462032	-0.98495
C	-9.271809	1.55321	-1.221959
C	-8.521954	0.871082	-0.30737
S	-9.535636	0.121141	0.883643
C	-7.046586	0.882039	-0.203735
C	-6.211919	-0.230811	-0.280908
C	-4.815188	-0.081819	-0.103186
C	-4.235094	1.185519	0.127602
C	-5.098729	2.301263	0.165451
C	-6.453733	2.144656	0.009394
C	-3.950796	-1.20161	-0.141216
C	-2.600317	-1.041287	-0.01029
C	-1.98666	0.227796	0.186696
C	-2.830755	1.335636	0.30122
C	-4.482464	-2.567403	-0.360925
C	-6.74113	-1.580459	-0.628856
N	-5.853659	-2.657333	-0.588058
C	-4.573197	3.668764	0.393768
C	-2.328013	2.671862	0.718859
N	-3.214202	3.756513	0.651214
C	-6.426527	-3.968538	-0.883088
C	-2.649529	5.061635	0.988077
O	-5.293074	4.650685	0.375961
O	-1.20253	2.867627	1.128308
O	-7.896216	-1.780595	-0.948575
O	-3.771403	-3.553493	-0.355729
H	-1.975101	-1.921267	-0.097829
H	-7.081047	3.026255	0.067826
H	-11.416757	1.945366	-1.602323
H	-8.833761	2.103805	-2.046173
H	-14.454735	-0.43892	3.080659

H	-11.885143	-0.025177	2.754095
H	-3.413443	5.810246	0.796385
H	-2.351207	5.08279	2.038172
H	-1.764432	5.243138	0.377864
H	-7.256195	-4.167033	-0.203379
H	-6.808547	-3.988264	-1.905545
H	-5.639414	-4.706955	-0.757428
C	-0.520855	0.21292	0.190008
C	0.254676	-0.776829	0.746271
C	1.631207	-0.654189	0.463258
C	1.920312	0.415806	-0.350653
S	0.479063	1.312295	-0.71419
C	3.204423	0.828421	-0.873869
C	3.465426	1.653566	-1.937593
C	4.849152	1.820918	-2.185565
C	5.651285	1.111583	-1.330819
S	4.687023	0.254327	-0.170766
H	-0.158822	-1.574037	1.353913
H	2.386614	-1.344736	0.817593
H	2.68662	2.107527	-2.540701
H	5.253222	2.430652	-2.984504
C	7.122241	1.192232	-1.24607
C	8.014699	0.086327	-1.27842
C	9.39912	0.293775	-1.076309
C	9.931503	1.608196	-0.877639
C	9.020014	2.686996	-0.918301
C	7.653061	2.461984	-1.083111
C	10.306715	-0.787983	-1.076514
C	11.661541	-0.572507	-0.841726
C	12.19859	0.689866	-0.618339
C	11.319521	1.815618	-0.666418
C	9.474523	4.06293	-0.768711
C	11.804629	3.195925	-0.584251
N	10.85007	4.223194	-0.617299
C	7.55053	-1.261058	-1.613553
C	9.851266	-2.154926	-1.299265
N	8.487669	-2.298853	-1.560863
O	6.399873	-1.534706	-1.941623
O	10.596437	-3.130613	-1.278979
O	8.720558	5.03272	-0.782863
O	12.983825	3.524444	-0.494395
C	7.977578	-3.629045	-1.859535
C	11.377491	5.575915	-0.510872

H	6.999461	3.325562	-1.049952
H	12.293943	-1.451634	-0.801062
H	7.582575	-3.660767	-2.877531
H	8.803212	-4.326878	-1.746139
H	7.162081	-3.875943	-1.176839
H	10.530787	6.257053	-0.533902
H	11.939056	5.685326	0.419238
H	12.060715	5.778511	-1.338447
C	13.634522	0.736814	-0.294398
C	14.302901	1.386542	0.711189
C	15.677335	1.07624	0.772066
C	16.087383	0.188342	-0.193512
S	14.740688	-0.264091	-1.195475
C	17.40728	-0.350178	-0.42073
C	17.787885	-1.353905	-1.282707
C	19.164659	-1.648798	-1.215707
C	19.865261	-0.85688	-0.336143
S	18.78518	0.265838	0.439071
H	13.813903	2.080838	1.378867
H	16.34857	1.489376	1.517534
H	17.090315	-1.872411	-1.929182
H	19.636661	-2.421038	-1.8129
C	21.265747	-1.057936	0.044998
C	21.657132	-2.421255	0.190022
C	22.89451	-2.789959	0.636312
C	23.838458	-1.804034	0.999764
C	23.496453	-0.444349	0.838964
C	22.220264	-0.07479	0.328325
C	24.456924	0.525838	1.208088
C	25.684472	0.152599	1.714244
C	26.013729	-1.200006	1.866134
C	25.099398	-2.167052	1.509621
C	25.448815	-3.599995	1.664004
C	23.221368	-4.231661	0.773798
C	24.166436	1.970474	1.056466
C	22.002389	1.359546	0.005356
N	24.487726	-4.535711	1.284079
N	22.950577	2.284908	0.466761
O	21.064686	1.767974	-0.648628
O	24.954098	2.830789	1.408189
O	22.439273	-5.108137	0.461696
O	26.52349	-3.969498	2.09908
H	20.937191	-3.201345	-0.024846

H	26.976104	-1.507451	2.258457
H	26.382769	0.934976	1.98819
C	22.650114	3.688894	0.195302
C	24.85772	-5.939298	1.443409
H	21.657148	3.928887	0.576434
H	23.410342	4.289228	0.68756
H	22.656729	3.87399	-0.880769
H	24.016876	-6.54244	1.111939
H	25.745624	-6.157993	0.847568
H	25.08816	-6.144299	2.490286
SCF Energy = -8513.18755722 Hartree			
Spin Contamination <S2> = 0.7768			

Table S3. TD-B3LYP/6-31G** vertical electronic transitions for $(NDI2OD\text{-}T2)_4$, neutral species

TD-B3LYP/6-31G neutral**				
Excited State 1:	**1.6307 eV**	**760.30 nm**	**f= 1.9037**	**<S**2>=0.000**
Excited State 2:	1.7366 eV	713.95 nm	f= 0.0164	<S**2>=0.000
Excited State 3:	1.8175 eV	682.18 nm	f= 0.0863	<S**2>=0.000
Excited State 4:	1.8690 eV	663.35 nm	f= 0.0161	<S**2>=0.000
Excited State 5:	1.8752 eV	661.19 nm	f= 0.0057	<S**2>=0.000
Excited State 6:	1.9316 eV	641.86 nm	f= 0.0506	<S**2>=0.000
Excited State 7:	1.9627 eV	631.70 nm	f= 0.0069	<S**2>=0.000
Excited State 8:	1.9961 eV	621.14 nm	f= 0.0099	<S**2>=0.000
Excited State 9:	2.0428 eV	606.93 nm	f= 0.0074	<S**2>=0.000
Excited State 10:	2.0583 eV	602.36 nm	f= 0.0082	<S**2>=0.000

Table S4. TD-CAM-B3LYP/6-31G** vertical electronic transitions for $(NDI2OD\text{-}T2)_4$, neutral species

TD-CAMB3LYP/6-31G neutral**				
Excited State 1:	**2.6543 eV**	**467.11 nm**	**f= 1.5716**	**<S**2>=0.000**
Excited State 2:	2.7388 eV	452.70 nm	f= 0.3500	<S**2>=0.000
Excited State 3:	2.8145 eV	440.52 nm	f= 0.0126	<S**2>=0.000
Excited State 4:	2.9090 eV	426.21 nm	f= 0.0364	<S**2>=0.000
Excited State 5:	2.9470 eV	420.72 nm	f= 0.0041	<S**2>=0.000
Excited State 6:	2.9929 eV	414.26 nm	f= 0.0054	<S**2>=0.000
Excited State 7:	3.0144 eV	411.31 nm	f= 0.0068	<S**2>=0.000
Excited State 8:	3.7682 eV	329.03 nm	f= 0.2773	<S**2>=0.000
Excited State 9:	3.7718 eV	328.71 nm	f= 0.5074	<S**2>=0.000
Excited State 10:	3.7737 eV	328.55 nm	f= 0.2624	<S**2>=0.000

Table S5. TD-UCAM-B3LYP/6-31G** vertical electronic transitions for $(NDI2OD\text{-}T2)_4$, charged species

TD-CAMB3LYP/6-31G charged species (-1)**				
Excited State 1:	0.3711 eV	3341.21 nm	f= 0.0035	<S**2>=0.785
Excited State 2:	0.5364 eV	2311.62 nm	f= 0.0971	<S**2>=0.806
Excited State 3:	0.6254 eV	1982.62 nm	f= 0.1210	<S**2>=0.844
Excited State 4:	1.5169 eV	817.33 nm	f= 0.0035	<S**2>=2.576
Excited State 5:	1.5518 eV	798.98 nm	f= 0.0013	<S**2>=2.707
Excited State 6:	**1.8332 eV**	**676.34 nm**	**f= 0.4835**	**<S**2>=0.997**
Excited State 7:	1.8575 eV	667.47 nm	f= 0.0004	<S**2>=2.775
Excited State 8:	**1.9907 eV**	**622.81 nm**	**f= 0.1548**	**<S**2>=1.319**
Excited State 9:	**2.0790 eV**	**596.37 nm**	**f= 0.3248**	**<S**2>=1.995**
Excited State 10:	2.1230 eV	584.02 nm	f= 0.0159	<S**2>=1.992
Excited State 11:	2.1467 eV	577.56 nm	f= 0.3919	<S**2>=1.464
Excited State 12:	2.1708 eV	571.16 nm	f= 0.0278	<S**2>=1.248
Excited State 13:	2.2212 eV	558.19 nm	f= 0.0031	<S**2>=2.617
Excited State 14:	2.2401 eV	553.47 nm	f= 0.0044	<S**2>=0.919
Excited State 15:	2.2734 eV	545.38 nm	f= 0.0059	<S**2>=1.452
Excited State 16:	2.2906 eV	541.28 nm	f= 0.0008	<S**2>=1.768
Excited State 17:	2.3100 eV	536.73 nm	f= 0.0007	<S**2>=0.788
Excited State 18:	2.3272 eV	532.77 nm	f= 0.0405	<S**2>=1.273
Excited State 19:	2.3521 eV	527.13 nm	f= 0.0000	<S**2>=2.776
Excited State 20:	2.4586 eV	504.30 nm	f= 0.0040	<S**2>=2.324
Excited State 21:	2.5071 eV	494.54 nm	f= 0.0201	<S**2>=1.460
Excited State 22:	2.5160 eV	492.79 nm	f= 0.0022	<S**2>=1.763
Excited State 23:	2.5473 eV	486.72 nm	f= 0.0292	<S**2>=1.032
Excited State 24:	2.5866 eV	479.33 nm	f= 0.0176	<S**2>=0.873
Excited State 25:	2.6409 eV	469.48 nm	f= 0.0007	<S**2>=2.728
Excited State 26:	2.6421 eV	469.27 nm	f= 0.3344	<S**2>=1.138
Excited State 27:	2.6632 eV	465.55 nm	f= 0.0734	<S**2>=1.550
Excited State 28:	2.7292 eV	454.30 nm	f= 0.0180	<S**2>=0.892
Excited State 29:	2.7444 eV	451.78 nm	f= 0.0282	<S**2>=1.879
Excited State 30:	2.7890 eV	444.54 nm	f= 0.0258	<S**2>=1.616
Excited State 31:	2.7901 eV	444.37 nm	f= 0.0445	<S**2>=0.966
Excited State 32:	2.8439 eV	435.96 nm	f= 0.0510	<S**2>=1.218
Excited State 33:	2.8557 eV	434.17 nm	f= 0.0015	<S**2>=1.785
Excited State 34:	2.8782 eV	430.77 nm	f= 0.0003	<S**2>=2.589
Excited State 35:	2.8871 eV	429.44 nm	f= 0.0151	<S**2>=2.062
Excited State 36:	2.9141 eV	425.47 nm	f= 0.0274	<S**2>=1.680

Excited State 37:	2.9583 eV	419.11 nm	f= 0.0200	<S**2>=0.868
Excited State 38:	2.9739 eV	416.91 nm	f= 0.0383	<S**2>=0.778
Excited State 39:	3.0248 eV	409.89 nm	f= 0.0072	<S**2>=2.696
Excited State 40:	3.0768 eV	402.97 nm	f= 0.1928	<S**2>=1.247
Excited State 41:	3.1102 eV	398.64 nm	f= 0.0120	<S**2>=1.003
Excited State 42:	3.1308 eV	396.01 nm	f= 0.0446	<S**2>=1.831
Excited State 43:	3.1556 eV	392.91 nm	f= 0.0555	<S**2>=0.979
Excited State 44:	3.1625 eV	392.05 nm	f= 0.1172	<S**2>=1.952
Excited State 45:	3.1738 eV	390.65 nm	f= 0.0308	<S**2>=2.186
Excited State 46:	3.2100 eV	386.25 nm	f= 0.0198	<S**2>=1.293
Excited State 47:	3.2583 eV	380.52 nm	f= 0.0353	<S**2>=1.215
Excited State 48:	3.2707 eV	379.07 nm	f= 0.0348	<S**2>=1.964
Excited State 49:	3.2942 eV	376.37 nm	f= 0.0084	<S**2>=2.309
Excited State 50:	3.3253 eV	372.85 nm	f= 0.0056	<S**2>=2.172

Table S6. Single occupied/unoccupied molecular orbitals involved in the $S^-_0 \rightarrow S^-_6$ transition for the charged species

Orbital	Contribution
470A -> 477A	-0.1754
470A -> 478A	-0.11259
470A -> 479A	-0.43336
470A -> 481A	0.22149
470A -> 484A	0.2449
470A -> 485A	**0.51329**
470A -> 486A	-0.14993
470A -> 488A	-0.40431
470A -> 495A	0.11637
468B -> 472B	0.13809
469B -> 472B	0.17316

Table S7. Single occupied/unoccupied molecular orbitals isosurfaces involved in the $S^-_0 \rightarrow S^-_6$ transition for the charged species

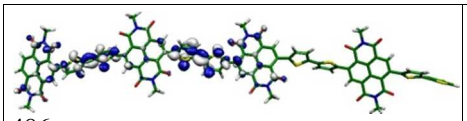 486a	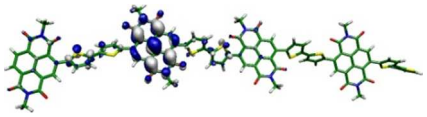 488a	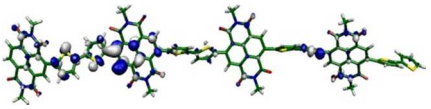 495a
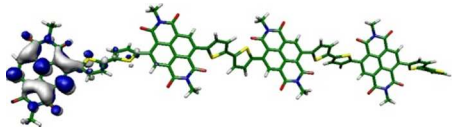 481a	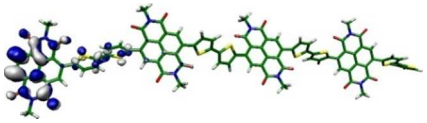 484a	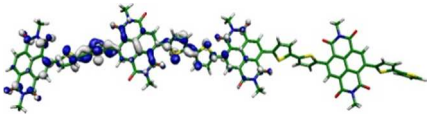 **485a**
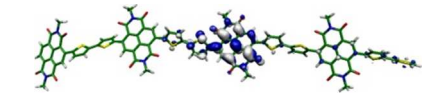 477 a	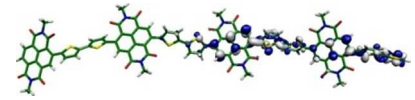 478 a	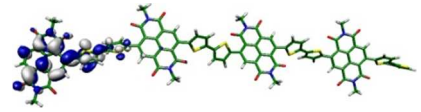 479a
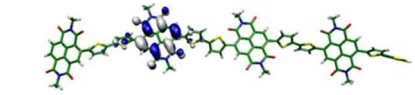 **470a**	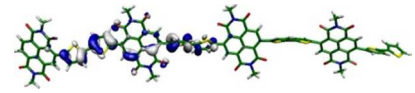 468b	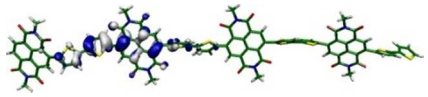 469b

Table S8. TD-UCAM-B3LYP/6-31G** vertical electronic transitions for $(NDI2OD\text{-}T2)_5$, charged species

TD-UCAM-B3LYP/6-31G (charged species), n=5**				
Excited State 1:	0.4410 eV	2811.25 nm	f= 0.0045	<S**2>=0.786
Excited State 2:	0.4528 eV	2737.98 nm	f= 0.0489	<S**2>=0.795
Excited State 3:	0.5617 eV	2207.27 nm	f= 0.2142	<S**2>=0.842
Excited State 4:	0.5915 eV	2096.14 nm	f= 0.0365	<S**2>=0.814
Excited State 5:	1.4284 eV	867.98 nm	f= 0.0097	<S**2>=2.599
Excited State 6:	1.4943 eV	829.70 nm	f= 0.0025	<S**2>=2.709
Excited State 7:	1.7658 eV	702.15 nm	f= 0.0000	<S**2>=2.777
Excited State 8:	**1.7976 eV**	**689.74 nm**	**f= 0.5559**	**<S**2>=1.035**
Excited State 9:	1.8699 eV	663.04 nm	f= 0.0500	<S**2>=2.690
Excited State 10:	**1.9776 eV**	**626.96 nm**	**f= 0.3548**	**<S**2>=1.320**
Excited State 11:	**2.0472 eV**	**605.63 nm**	**f= 0.3941**	**<S**2>=1.324**
Excited State12:	2.0864 eV	594.24 nm	f= 0.2012	<S**2>=2.002
Excited State 13:	2.1409 eV	579.13 nm	f= 0.0305	<S**2>=2.429
Excited State 14:	2.1768 eV	569.57 nm	f= 0.2978	<S**2>=1.276
Excited State 15:	2.1956 eV	564.71 nm	f= 0.0616	<S**2>=2.428
Excited State 16:	2.2310 eV	555.73 nm	f= 0.0228	<S**2>=1.731
Excited State 17:	2.2380 eV	554.01 nm	f= 0.0001	<S**2>=0.788
Excited State 18:	2.2520 eV	550.56 nm	f= 0.0074	<S**2>=1.714
Excited State 19:	2.2621 eV	548.10 nm	f= 0.0033	<S**2>=1.546
Excited State 20:	2.2990 eV	539.29 nm	f= 0.0006	<S**2>=2.714
Excited State 21:	2.3166 eV	535.19 nm	f= 0.0164	<S**2>=0.916
Excited State 22:	2.3169 eV	535.12 nm	f= 0.0397	<S**2>=1.290
Excited State 23:	2.3591 eV	525.56 nm	f= 0.0037	<S**2>=1.718
Excited State 24:	2.3747 eV	522.11 nm	f= 0.0003	<S**2>=1.772
Excited State 25:	2.4440 eV	507.30 nm	f= 0.0109	<S**2>=2.263
Excited State 26:	2.5102 eV	493.92 nm	f= 0.0126	<S**2>=1.816
Excited State 27:	2.5134 eV	493.29 nm	f= 0.0408	<S**2>=1.658
Excited State 28:	2.5305 eV	489.95 nm	f= 0.0188	<S**2>=0.955
Excited State 29:	2.5511 eV	486.00 nm	f= 0.0102	<S**2>=0.891
Excited State 30:	2.5820 eV	480.18 nm	f= 0.0897	<S**2>=1.625

Table S9. Optimized geometry for the charged (-1) molecular dimer, UM06-2X/6-311G** level of theory

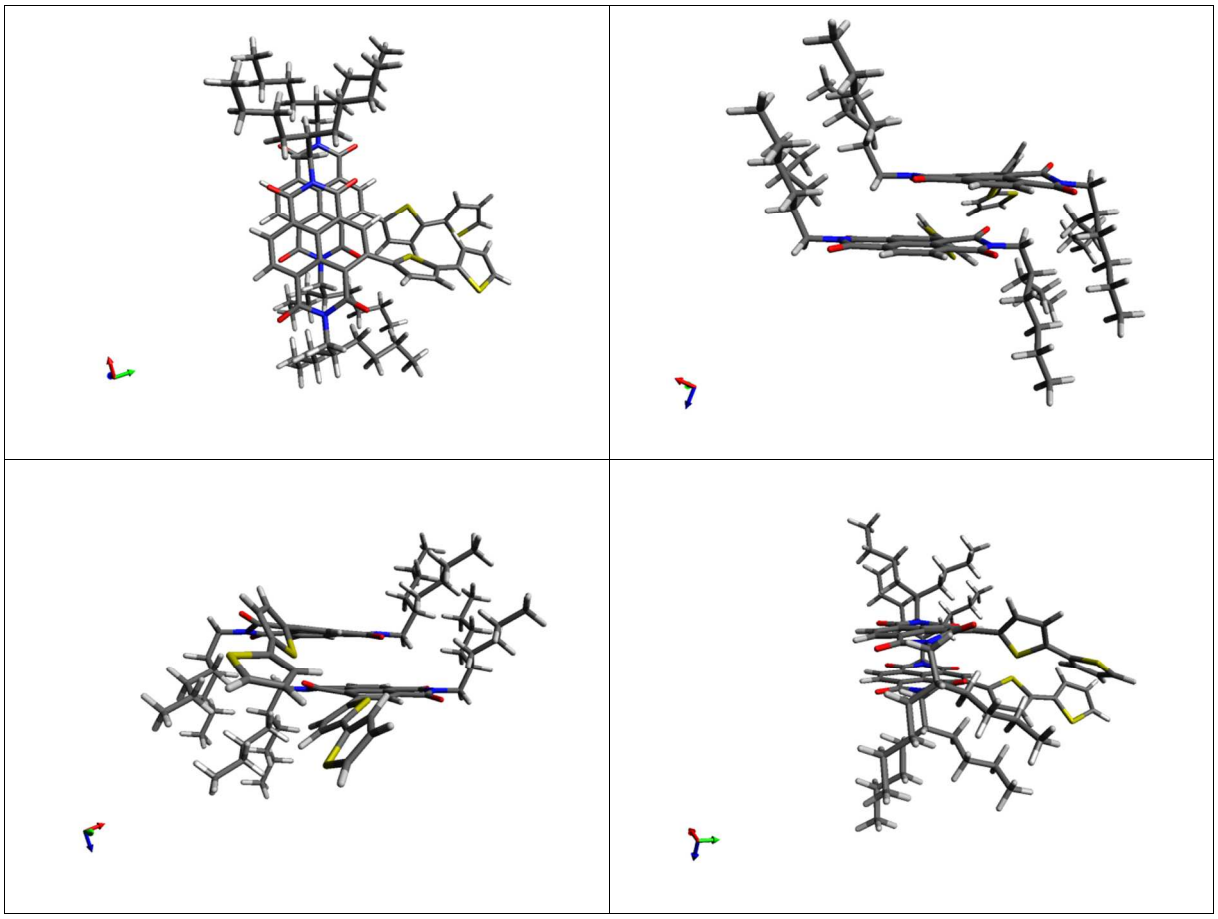

Table S10. TD-CAM-B3LYP and TD-UCAM-B3LYP/6-31G** vertical electronic transitions computed for the optimized neutral and charged molecular dimer

TD-UCAM-B3LYP (neutral dimer)				
Excited State 1:	2.8313 eV	437.91 nm	f= 0.0008	<S**2>=0.000
Excited State 2:	**2.9819 eV**	**415.78 nm**	**f= 0.7022**	**<S**2>=0.000**
Excited State 3:	3.2879 eV	377.09 nm	f= 0.0037	<S**2>=0.000
Excited State 4:	3.4245 eV	362.05 nm	f= 0.0006	<S**2>=0.000
Excited State 5:	3.7167 eV	333.59 nm	f= 0.0222	<S**2>=0.000
Excited State 6:	3.7935 eV	326.84 nm	f= 0.0013	<S**2>=0.000
Excited State 7:	3.8379 eV	323.05 nm	f= 0.0321	<S**2>=0.000
Excited State 8:	3.8607 eV	321.14 nm	f= 0.4930	<S**2>=0.000
Excited State 9:	3.9889 eV	310.82 nm	f= 0.0095	<S**2>=0.000
Excited State 10:	4.0078 eV	309.36 nm	f= 0.0028	<S**2>=0.000
Excited State 11:	4.0130 eV	308.96 nm	f= 0.0092	<S**2>=0.000
Excited State 12:	4.1112 eV	301.57 nm	f= 0.7522	<S**2>=0.000
Excited State 13:	4.1371 eV	299.69 nm	f= 0.0191	<S**2>=0.000
Excited State 14:	4.1523 eV	298.59 nm	f= 0.0023	<S**2>=0.000
Excited State 15:	4.2898 eV	289.02 nm	f= 0.0642	<S**2>=0.000
TD-UCAM-B3LYP (charged dimer)				
Excited State 1:	0.7316 eV	1694.62 nm	f= 0.0667	<S**2>=0.801
Excited State 2:	**1.7916 eV**	**692.03 nm**	**f= 0.0718**	**<S**2>=1.149**
Excited State 3:	2.0373 eV	608.57 nm	f= 0.0235	<S**2>=2.352
Excited State 4:	2.0600 eV	601.88 nm	f= 0.0269	<S**2>=1.602
Excited State 5:	2.2079 eV	561.55 nm	f= 0.0253	<S**2>=0.988
Excited State 6:	2.4337 eV	509.45 nm	f= 0.0137	<S**2>=2.142
Excited State 7:	2.4891 eV	498.10 nm	f= 0.0202	<S**2>=1.969
Excited State 8:	2.6073 eV	475.53 nm	f= 0.0017	<S**2>=0.897
Excited State 9:	2.7010 eV	459.04 nm	f= 0.0727	<S**2>=1.026
Excited State 10:	2.8885 eV	429.24 nm	f= 0.0213	<S**2>=2.281
Excited State 11:	2.9071 eV	426.49 nm	f= 0.1296	<S**2>=1.254
Excited State 12:	2.9539 eV	419.74 nm	f= 0.0873	<S**2>=1.066
Excited State 13:	3.0510 eV	406.37 nm	f= 0.0024	<S**2>=1.747
Excited State 14:	3.0949 eV	400.61 nm	f= 0.0788	<S**2>=1.242
Excited State 15:	3.1451 eV	394.21 nm	f= 0.0526	<S**2>=1.356
Excited State 16:	3.1989 eV	387.58 nm	f= 0.1647	<S**2>=0.951
Excited State 17:	3.2870 eV	377.20 nm	f= 0.0137	<S**2>=1.150
Excited State 18:	3.4251 eV	361.99 nm	f= 0.0004	<S**2>=2.592
Excited State 19:	3.4742 eV	356.87 nm	f= 0.0188	<S**2>=2.087
Excited State 20:	3.5313 eV	351.10 nm	f= 0.0026	<S**2>=2.084

Excited State 21:	3.5510 eV	349.15 nm	f= 0.0016	<S**2>=1.759
Excited State 22:	3.5855 eV	345.79 nm	f= 0.0044	<S**2>=1.755
Excited State 23:	3.6068 eV	343.75 nm	f= 0.0360	<S**2>=1.782
Excited State 24:	3.6251 eV	342.01 nm	f= 0.0416	<S**2>=1.729
Excited State 25:	3.6427 eV	340.36 nm	f= 0.0173	<S**2>=2.036
Excited State 26:	3.6732 eV	337.54 nm	f= 0.0031	<S**2>=1.401
Excited State 27:	3.7786 eV	328.12 nm	f= 0.0284	<S**2>=1.565
Excited State 28:	3.7999 eV	326.29 nm	f= 0.0055	<S**2>=1.911
Excited State 29:	3.8281 eV	323.88 nm	f= 0.0654	<S**2>=1.267
Excited State 30:	3.8799 eV	319.55 nm	f= 0.2563	<S**2>=1.095

Table S11. TD-CAM-B3LYP and TD-UCAM-B3LYP/6-31G** vertical electronic transitions computed for one monomer as extracted from the optimized neutral and charged molecular dimer

TD-UCAMB3LYP (neutral monomer)				
Excited State 1:	**2.9560 eV**	**419.44 nm**	**f= 0.4664**	**<S**2>=0.000**
Excited State 2:	3.8583 eV	321.34 nm	f= 0.3183	<S**2>=0.000
Excited State 3:	3.9722 eV	312.13 nm	f= 0.0161	<S**2>=0.000
Excited State 4:	4.0679 eV	304.79 nm	f= 0.4987	<S**2>=0.000
Excited State 5:	4.1396 eV	299.51 nm	f= 0.0068	<S**2>=0.000
Excited State 6:	4.2452 eV	292.06 nm	f= 0.0418	<S**2>=0.000
Excited State 7:	4.3601 eV	284.36 nm	f= 0.0046	<S**2>=0.000
Excited State 8:	4.3724 eV	283.56 nm	f= 0.0392	<S**2>=0.000
Excited State 9:	4.5455 eV	272.76 nm	f= 0.0235	<S**2>=0.000
Excited State 10:	4.5942 eV	269.87 nm	f= 0.0009	<S**2>=0.000
Excited State 11:	4.7664 eV	260.12 nm	f= 0.0496	<S**2>=0.000
Excited State 12:	4.8924 eV	253.42 nm	f= 0.0392	<S**2>=0.000
Excited State 13:	5.0326 eV	246.36 nm	f= 0.0052	<S**2>=0.000
Excited State 14:	5.1006 eV	243.08 nm	f= 0.0489	<S**2>=0.000
Excited State 15:	5.3011 eV	233.88 nm	f= 0.0364	<S**2>=0.000
TD-UCAMB3LYP (charged monomer)				
Excited State 1:	1.7203 eV	720.72 nm	f= 0.1022	<S**2>=1.164
Excited State 2:	**2.0386 eV**	**608.17 nm**	**f= 0.0407**	**<S**2>=1.315**
Excited State 3:	2.2409 eV	553.27 nm	f= 0.0346	<S**2>=1.256
Excited State 4:	2.5282 eV	490.40 nm	f= 0.0446	<S**2>=1.288
Excited State 5:	2.8819 eV	430.22 nm	f= 0.2347	<S**2>=1.134
Excited State 6:	3.0048 eV	412.62 nm	f= 0.1741	<S**2>=1.052
Excited State 7:	3.2264 eV	384.28 nm	f= 0.1275	<S**2>=1.127
Excited State 8:	3.4893 eV	355.32 nm	f= 0.0477	<S**2>=2.213
Excited State 9:	3.6095 eV	343.49 nm	f= 0.0233	<S**2>=1.918
Excited State 10:	3.7151 eV	333.73 nm	f= 0.0037	<S**2>=1.145
Excited State 11:	3.8531 eV	321.78 nm	f= 0.5050	<S**2>=0.909
Excited State 12:	3.9750 eV	311.91 nm	f= 0.0181	<S**2>=1.251
Excited State 13:	4.0655 eV	304.97 nm	f= 0.0176	<S**2>=2.230
Excited State 14:	4.1133 eV	301.42 nm	f= 0.0004	<S**2>=1.196
Excited State 15:	4.1525 eV	298.57 nm	f= 0.0085	<S**2>=1.723
Excited State 16:	4.2233 eV	293.57 nm	f= 0.0032	<S**2>=1.170
Excited State 17:	4.2997 eV	288.36 nm	f= 0.0055	<S**2>=1.748
Excited State 18:	4.3425 eV	285.51 nm	f= 0.0041	<S**2>=1.523
Excited State 19:	4.3949 eV	282.11 nm	f= 0.0196	<S**2>=1.803

Excited State 20:	4.4080 eV	281.27 nm	f= 0.0601	<S**2>=1.684
Excited State 21:	4.4705 eV	277.34 nm	f= 0.0042	<S**2>=2.229
Excited State 22:	4.4814 eV	276.66 nm	f= 0.0277	<S**2>=1.315
Excited State 23:	4.5763 eV	270.93 nm	f= 0.0332	<S**2>=1.917
Excited State 24:	4.6162 eV	268.58 nm	f= 0.0004	<S**2>=1.209
Excited State 25:	4.7160 eV	262.90 nm	f= 0.0007	<S**2>=1.406
Excited State 26:	4.7540 eV	260.80 nm	f= 0.0150	<S**2>=1.167
Excited State 27:	4.7607 eV	260.43 nm	f= 0.0001	<S**2>=1.420
Excited State 28:	4.8761 eV	254.27 nm	f= 0.0113	<S**2>=1.317
Excited State 29:	4.9854 eV	248.70 nm	f= 0.0321	<S**2>=1.248
Excited State 30:	5.0123 eV	247.36 nm	f= 0.0150	<S**2>=1.134

Table S12. Single occupied/unoccupied molecular orbitals involved in the $S^-_0 \rightarrow S^-_2$ transition for the charged molecular dimer

Orbital	Contribution
380A -> 383A	-0.24571
381A -> 383A	**0.78624**
381A -> 384A	-0.12977
381A -> 385A	-0.18378
381A -> 386A	-0.26780
381A -> 389A	-0.13022
381A -> 390A	-0.12358
378B -> 383B	0.10130
380B -> 382B	0.16101
380B -> 383B	-0.19841

Table S13. Single occupied/unoccupied molecular orbitals isosurfaces involved in the $S^-_0 \rightarrow S^-_2$ transition for the charged molecular dimer

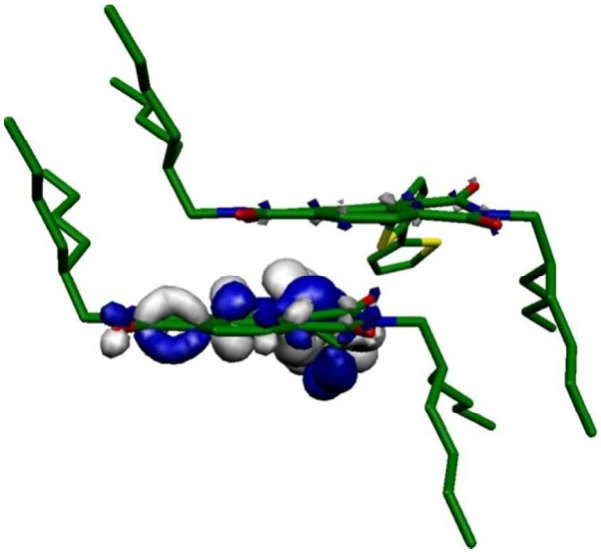

383A (lateral view)

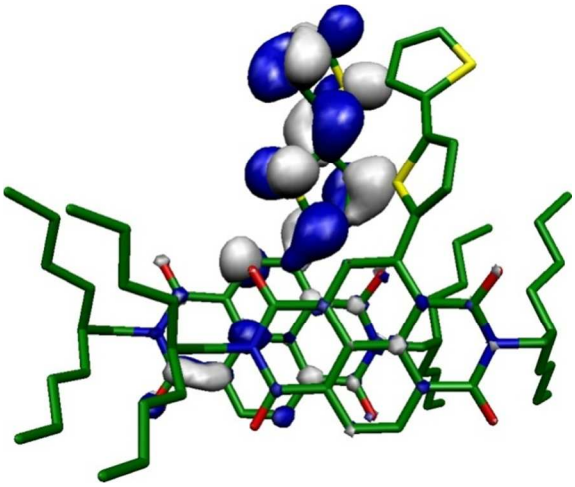

383A (top view)

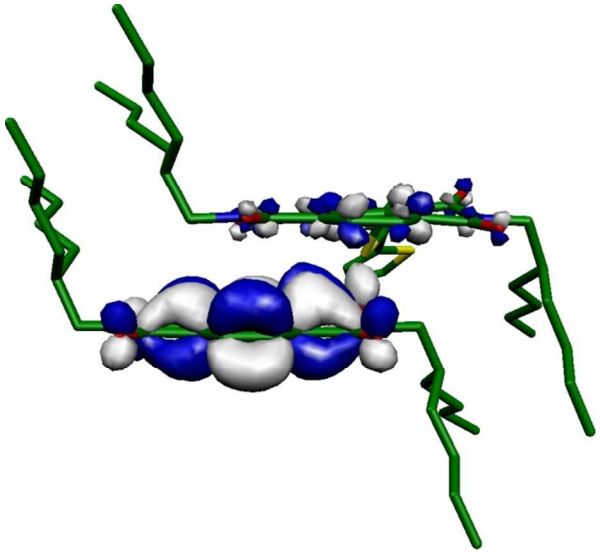

381A (lateral view)

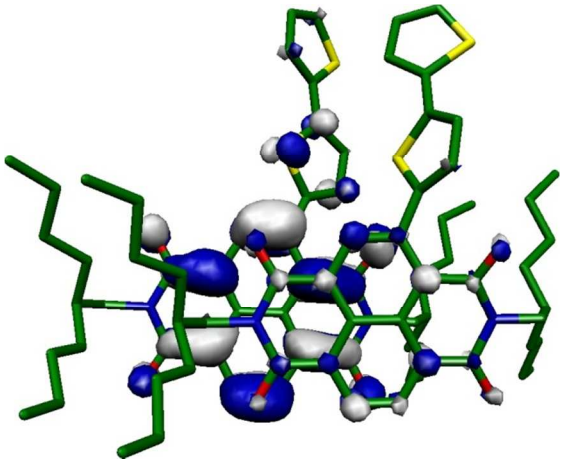

381A (top view)